Hindawi
Journal of Applied Mathematics
Volume 2023, Article ID 5591165, 19 pages
https://doi.org/10.1155/2023/5591165

Research Article

Modeling and Optimal Control Analysis Applied to Real Cases of COVID-19 Pandemic with Double Dose Vaccination in Ethiopia

Fekadu Mosisa Legesse, Koya Purnachandra Rao, and Temesgen Duressa Keno

Department of Mathematics, Wollega University, Nekemte, Ethiopia

Correspondence should be addressed to Fekadu Mosisa Legesse; fekadumosisa22@gmail.com

Received 25 February 2023; Revised 28 May 2023; Accepted 19 June 2023; Published 20 July 2023

Academic Editor: Qiankun Song

The novel coronavirus is a recently discovered member of one of the largest families of viruses with symptoms ranging from a simple cold to excruciating respiratory agony. In the present paper, a deterministic mathematical model is formulated to estimate the transmission dynamics of COVID-19 with the inclusion of control strategies like (i) double-dose vaccination, (ii) prevention, and (iii) treatment. In addition, instead of considering all infectious humans as one unit, we separate them into symptomatic and asymptomatic groups, and the impact is analyzed. This separation is meaningful because various reports indicate that the asymptomatic cases will spread the disease more than the symptomatic cases. The model is proved to be mathematically well-posed and biologically meaningful by showing positivity and boundedness of the solution using the appropriate initial conditions. For the reproduction number, a parametric formula is constructed, and also the associated numerical value is calculated from the reported real data in Ethiopia. Moreover, disease-free and endemic equilibria are determined, and their local and global stabilities are discussed using the Lyapunov function technique. These equilibria are found to be locally asymptotically stable if $R_0 < 1$ and $R_0 > 1$, respectively. Following the model fitting and estimation of the parameter values, sensitivity analysis was performed in order to analyze the impact of each parameter on transmission dynamics. In other words, this study can be used to evaluate how major model parameters affect transmission dynamics and control. Utilizing Pontryagin's maximal principle, the best control measures are implemented with the aim of lowering the burdens associated with infection, prevention, and treatment. To comprehend and visualize the impact of control techniques on the development of the disease and to illustrate the analytical findings generated in this study, numerical simulation studies are conducted. Finally, the output of the study illustrates that adhering to all the control strategies has a big impact on minimizing the transmission of the disease in society. Which means that if the control strategies are well managed by the concerned body, then the burden of the disease is reduced quickly in the Ethiopian population.

1. Introduction

The novel coronavirus (COVID-19) is one of the largest fatal viruses which infected millions of humans throughout the world within a short period of time and has posed serious challenges to human life style including the economy and GDPs of the developed countries. The outbreak of the COVID-19 pandemic was first declared by the People's Republic of China on 31st December 2019, and it appeared in China, Wuhan City [1]. The infection caused by COVID-19 is identified by its signs and symptoms. Most of the signs and symptoms of COVID-19 are similar to the common cold illness, but it is more dangerous and causes severe respiratory problems. Despite efforts being made to curb the transmission of the COVID-19 disease, the disease is still persistent or endemic in many parts of the globe including Ethiopia [2]. Hence, globally, human beings are still facing a health problem due to the coronavirus. Numerous studies indicate that direct human contact or physical separation between susceptible individuals is the primary means of spreading this epidemic [3, 4]. This is why COVID-19 becomes pandemic within a very short duration

of time and is difficult to mitigate but reduce the transmission rate due the corresponding vaccine is obtained.

According to the nature of its mutation rate and the criticality of the virus, COVID-19 causes millions of deaths throughout the globe. Because of this, the World Health Organization (WHO) and scientists throughout the world face a lot of challenges and competition to get the corresponding vaccine. But now, starting from 7 March 2022, 10 vaccines exist and are granted by the WHO for emergency use in the case of coronavirus [5]. Up to March 07, 2022, around 10.9 billion COVID-19 vaccine doses were managed globally, and 63.4% of the population throughout the world has taken the minimum of one dose of a vaccine. This coverage almost represents developed countries due to the shortage of the vaccine in developing countries. Up to the date mentioned above, only 13.6% of people in developing countries have received the minimum of one dose of the vaccine [6]. In Ethiopia, until 5 March 2022, 26,178,996 amount of vaccine doses had been administered [7].

A deterministic epidemiological model can be used to evaluate the dynamics of any infectious disease's transmission and outbreak as of the middle of the 20th century. This model represents real-world situations and predicts the severity of those diseases using the concept of mathematics [2]. A lot of research work has been conducted on the transmission dynamics of novel coronavirus and different models are also presented. Additionally, a number of research works have been interested to identify the best vaccination strategy to control the transmission of coronavirus [8, 9].

For instance, Matrajt et al. [10] presented a deterministic mathematical model depending on age to identify which group of age must be vaccinated first. They also verified that with low coverage, priority must be given to individuals whose age is 60 + years to reduce the number of mortality due to COVID-19. Semu et al. [11] developed a mathematical model to analyze the mitigation strategies for COVID-19 and take the following into account. The impact of asymptomatic patient individuals on the transmission rate of the disease in fully susceptible individuals, the effect of indirect spread of the disease through the population, and individuals behavioral changes in the community to use self-protective measures. Akuka et al. [12] formulated a SV_1V_2EIQR mathematical model with double-dose vaccination and quarantine to show that vaccination and treatment are very effective in controlling the spread of COVID-19 and that properly applying personal protective measures, that is, nonpharmaceutical public health interventions mechanisms such as proper use of face masks, regular hand washing, social distancing, and the like, should continue to be encouraged.

Since COVID-19 first arose in late 2019, numerous studies have been undertaken using mathematical models to begin studying the disease's transmission patterns and the pandemic's control mechanisms in various nations with the authors ([13–15]). For example, Atifa et al. [16] developed and examined a mathematical compartmental model for the pandemic's transmission patterns while accounting for the impact of human reinfection after complete recovery utilizing Pakistan COVID-19 genuine cases recorded. By comparing the growth rates of COVID-19 patients in Pakistan and Malaysia before and after the imposition of lockdown, a mathematical model based on Lotka-Volterra equations was created to shed light on the impact of lockdown on COVID-19 transmission dynamics, as presented by Abro et al. [17]. Coronavirus and diabetes relationships are discussed by the authors Ozkose et al. [18] using actual data from Turkey. In order to explore COVID-19 transmission and its connection to diabetes, a pandemic fractional order model is first developed. In their approach, both types of diabetes those with and without complications are taken into account in connection to the quarantine strategy. Peter et al. [19] developed and analyzed an epidemic model of COVID-19 governed by eight compartmental models. In their study, they also consider double-dose vaccination in order to control the transmission dynamic of the pandemic. In particular, their study's findings show that when vaccination rates rise, the number of infected individuals in the population declines, lowering the disease burden in Malaysia.

In addition, Sharbayta et al. [20] presented a $SV_1V_2EI_aI_s$ QHR deterministic mathematical model to conclude the transmission of COVID-19 in Ethiopia. In their study, they consider double-dose vaccination to mitigate the transmission of COVID-19 and use treatment strategy at quarantine and hospital classes to treat infected and critically ill individuals, respectively. By taking into account the combined effects of public health awareness, self-protective behavior, and treatment of hospitalized individuals, the authors [21–23] considered a deterministic mathematical model for the dynamics of COVID-19 transmission. This model is intended to reduce the spread of the disease. Additionally, by applying the combined effect least squares and Bayesian estimation mechanisms to the data gathered in Ethiopia and other nations, they calculate the unknown parameter values, identify the parameters that are most sensitive to the disease's transmission rate, and work to control its spread.

Therefore, the ongoing double-dose vaccination program and the two control techniques to slow the COVID-19 pandemic's spread among people are the driving forces behind this research. Here, we presented an optimal control analysis of the deterministic $SV_1V_2EI_aI_sR$ compartmental model to investigate the effect of prevention, treatment, and double doses of vaccination against novel coronavirus mitigation. The newly developed model is parameterized using the least squares method on daily reported COVID-19 confirmed cases in Ethiopia from 01 July, 2022, to 31 August 2022. After receiving the first and second doses of the immunization, the virus' transmission and progression are also determined.

The remaining parts of our manuscript are organized as below. The developed model is formulated in Section 2, its analytical analysis is explained in Section 3, and the estimation of the parameters using real data is discussed in Section 4. Sensitivity analysis is discussed in Section 5, and the extension of the proposed model into optimal control is elaborated in Section 6. The numerical simulations performed to support the analytical results discussed in Section 3 are presented in Section 7. Finally, a conclusion is presented.

2. Model Formulation

Mathematical modeling is one of the best mechanisms which is used to analyze the epidemiology of a disease. In

order to properly examine the transmission dynamics and control of the pandemic in the community, we design and analyze a deterministic mathematical model with the inclusion of control strategies and estimation of the parameters. According to their disease status at any moment t, the population size $N(t)$, which represents the suggested model, is divided into seven mutually exclusive individuals. These different classes include the number of susceptible humans $S(t)$, who are uninfected individuals with the disease but has a full chance to be infected with the diseases; the vaccinated individuals with the first dose $V_1(t)$, who still have a chance to be susceptible again and infected by COVID-19; the second dose vaccinated individuals $V_2(t)$, who are people those who have finished both dose vaccination within a time but still have a chance to be susceptible again due to waning vaccination during double dose vaccination time. As most of the researchers estimated, the vaccine will protect against 85 percent of infections with the most optimistic assumption. Hence, due to this, it is assumed that the population in the second dose of vaccinated humans goes to the recovered class at a rate Φ and the other moves to the susceptible class at a rate ϕ_2.The force of infection $\lambda = \beta((\omega I_a + I_s)/N)$, where β is the effective transmission rate and ω is the reduction in disease transmission in asymptomatic people. Since the considered population is assumed to be constant, the recruitment into the susceptible class is only through birth at the rate of Λ. Due to the first dose of the vaccine's inadequacy to prevent against COVID-19, susceptible humans enter the vaccinated compartment at a rate of θ after receiving the first dose, first-dose vaccinated humans enter the susceptible class at a rate of ϕ_1, and the remaining individuals enter the vaccinated compartment at a rate of ρ after receiving the second dose. The number of Exposed individuals $E(t)$ get infected without symptoms (asymptomatic) $I_a(t)$ or with symptoms (symptomatic) $I_s(t)$ at the rate of $p\nu$ and $(1-p)$ ν, respectively. Where ν is the progression rate from the incubation period (exposed class) to the infected classes, and p is a fraction of exposed individuals becoming infected asymptomatically while the remaining (1-p) fractions are infected symptomatically. γ_a and γ_s are the rates at which $I_a(t)$ and $I_s(t)$ are recovered from COVID-19 patient due to natural immunity and treatment of infected classes, respectively. $R(t)$ stands for the recovered compartment number; this class consists of either tested persons who have already had a COVID-19 negative result and are no longer in contact with contaminated areas or diseased individuals, or dead cases. In general, it is assumed that the size of the entire human population, indicated by $N(t)$, is constant and evenly distributed, as shown by:

$$N(t) = S(t) + V_1(t) + V_2(t) + E(t) + I_a(t) + I_s(t) + R(t). \tag{1}$$

The proposed COVID-19 model is governed by the following assumptions:

(i) All parameters are nonnegative

(ii) To keep the size of the population constant, consider all dead humans as newborns which are replaced in the susceptible class

(iii) The susceptible individuals are recruited by birth, and it is denoted by Λ through this manuscript

(iv) The death rate due to COVID-19 is considered in both symptomatic and asymptomatic classes as α_s and α_a, respectively.

(v) Full-dose vaccinated individuals become susceptible again due to waning vaccination

(vi) The recovered individuals have permanent immunity and have no probability of re-infection

(vii) The standard incidence rate $\lambda = \beta((\omega I_a + I_s)/N)$ can be used to represent the horizontal spread of infection

(viii) A proportion θ of susceptible individuals received first dose of vaccine

(ix) From the first dose-vaccinated individual, the ϕ_1 constant rate is moved to susceptible, whereas the remaining ρ rate of the individuals progresses out to the second-dose vaccinated individuals V_2

(x) Fully vaccinated populations are moved to the recovery class at a constant rate Φ

The proposed model considers first and second-dose vaccination as compartment with prevention and treatment as a control strategy to eradicate the transmission dynamics of coronavirus in Ethiopia. The proposed model parameters are described in Table 1 with their source. The model used in studying the transmission dynamics of COVID-19 in this study is governed by the next system of ordinary differential equation, i.e., Equation (2), while the corresponding flow diagram is depicted in Figure 1.

$$\begin{cases} \dfrac{dS}{dt} &= \Lambda + \phi_1 V_1 + \phi_2 V_2 - (\theta + \lambda + \mu)S, \\ \dfrac{dV_1}{dt} &= \theta S - (\mu + \rho + \phi_1)V_1, \\ \dfrac{dV_2}{dt} &= \rho V_1 - (\mu + \phi_2 + \Phi)V_2, \\ \dfrac{dE}{dt} &= \lambda S - (\mu + \nu)E, \\ \dfrac{dI_a}{dt} &= p\nu E - (\mu + \gamma_a + \alpha_a)I_a, \\ \dfrac{dI_s}{dt} &= (1-p)\nu E - (\mu + \gamma_s + \alpha_s)I_s, \\ \dfrac{dR}{dt} &= \gamma_a I_a + \gamma_s I_s + \Phi V_2 - \mu R, \end{cases} \tag{2}$$

Table 1: The model parameter estimation with their source.

Parameters	Description	Value	References
θ	Vaccination rate of first dose	0.11411	Fitted
Λ	Recruitment rate	121.317	Estimated
ϕ_1	Progression rate from V_1 to S	0.04348	Fitted
ϕ_2	Progression rate from V_2 to S	0.00076	Fitted
β	Transmission rate	0.98699	Fitted
μ	Natural mortality rate	$1/(67.8 * 365)$	Estimated
Φ	Recovery rate due to V_2	0.13191	Fitted
ν	Infection rate after incubation period	0.143	[23]
ρ	Second dose vaccination rate	0.03032	Fitted
α_a	Death rate of I_a individuals due to COVID-19	0.512	Fitted
α_s	COVID-19 induced death rate of I_s individuals	0.18219	[23]
ω	Modification factor for asymptomatic individuals	1	[23]
γ_s	Rate of recovery for an individuals with symptom	$1.89 * 10^{-7}$	[20]
γ_a	Rate of recovery for an asymptomatic individuals	0.0148	[20]
λ	Force of infection	0.0002176	Estimated
p	Fraction of infections that become asymptomatic	0.94744	Fitted
$\mathfrak{R}_c$	Effective reproduction number	0.00074951	Estimated
$\mathfrak{R}_0$	Reproduction number	2.105062463	Estimated

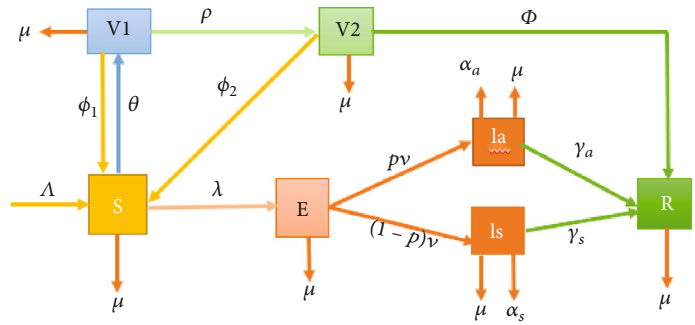

Figure 1: The schematic flow chart of COVID-19 transmission model.

subject to the next non-negative initial conditions

$$\begin{aligned} S(0) &> 0, \\ V_1(0) &\geq 0, \\ V_2(0) &\geq 0, \\ E(0) &\geq 0, \\ I_a(0) &\geq 0, \\ I_s(0) &\geq 0, \\ R(0) &\geq 0, \\ N(0) &> 0. \end{aligned} \tag{3}$$

Throughout this paper, $k_1 = \theta + \mu + \lambda$, $k_2 = \mu + \phi_1 + \rho$, $k_3 = \mu + \phi_2 + \Phi$, $k_4 = \mu + \nu$, $k_5 = \mu + \gamma_a + \alpha_a$, and $k_6 = \mu + \gamma_s + \alpha_s$.

3. Qualitative Analysis of the Model

In this section, some basic properties of the formulated model defined in Equation (2) including the feasible region, the positivity of the solution, equilibria, and their stability, are discussed.

3.1. Positivity and Boundedness of Solution

Theorem 1 (Positivity of the solutions). *Let* $F(t) = \{(S(t), V_1(t), V_2(t), E(t), I_a(t), I_s(t), R(t)) \in R_+^7 : S(0) > 0, V_1(0) \geq$

$0, V_2(0) \geq 0, E(0) \geq 0, I_a(0) \geq 0, I_s(0) \geq 0, R(0) \geq 0\}$, then the steady state set {S, V_1, V_2, E, I_a, I_s, and R} are all positive for all $t \geq 0$.

Proof. Choosing any one of equation from Equation (2) above, let us take the first equation i.e.,

$$\frac{dS}{dt} = \Lambda + \phi_1 V_1 + \phi_2 V_2 - (\theta + \lambda + \mu)S, \tag{4}$$

$$\frac{dS}{dt} \geq -(\theta + \lambda + \mu)S. \tag{5}$$

Integrating Equation (5) by separation of variable method, we obtain

$$S(t) \geq c_1 e^{-(\theta+\lambda+\mu)t}. \tag{6}$$

Using initial condition $S(0) = S_0$ and Equation (6), we obtain

$$S(t) \geq S_0 e^{-(\theta+\lambda+\mu)t} \geq 0 \text{ where } S_0 = e^{c_1}. \tag{7}$$

In a similar way, the remaining equations of Equation (2) can be proved and gives the following outputs:

$$\begin{aligned} V_1(t) &\geq V_1(0)e^{-(\rho+\phi_1+\mu)t} \geq 0, V_2(t) \geq V_2(0)e^{-(\Phi+\phi_2+\mu)t} \\ &\geq 0, E(t) \geq E_0 e^{-(\nu+\mu)t} \geq 0, \\ I_a(t) &\geq I_a(0)e^{-(\gamma_a+\alpha_a+\mu)t} \geq 0, I_s(t) \geq I_s(0)e^{-(\gamma_s+\alpha_s+\mu)t} \\ &\geq 0, R(t) \geq R_0 e^{-(\mu)t} \geq 0, \end{aligned} \tag{8}$$

which is the complete proof of the theorem. Hence, all solutions of Equation (2) are positive $\forall t \geq 0$. □

Theorem 2. *The region $\Omega = \{(S, V_1, V_2, E, I_a, I_s, R) \in R_+^7 : N(t) \leq (\Lambda/\mu)\}$ is positively invariant under the flow induced by the model Equation (2) which means the solution of the system should be well-posed and biologically meaningful in this region.*

Proof. From the total population size over a time t, we have

$$\frac{dN}{dt} = \frac{dS}{dt} + \frac{dV_1}{dt} + \frac{dV_2}{dt} + \frac{dE}{dt} + \frac{dI_a}{dt} + \frac{dI_s}{dt} + \frac{dR}{dt}, \tag{9}$$

$$\frac{dN}{dt} = \Lambda - \mu(S + V_1 + V_2 + E + I_a + I_s + R) - \alpha_a I_a - \alpha_s I_s. \tag{10}$$

Since $N(t)$ is assumed to be constant over a time t, then $(dN/dt) = 0$.

Hence, from Equation (1) and Equation (10), we obtain

$$\frac{dN}{dt} = \Lambda - \mu N - \alpha_a I_a - \alpha_s I_s = 0. \tag{11}$$

If death due to COVID-19 is zero, then Equation (11) becomes

$$\Lambda - \mu N \leq 0. \tag{12}$$

After some arrangement, Equation (12) becomes

$$N(t) \leq \frac{\Lambda}{\mu}. \tag{13}$$

Hence, each solution of Equation (2) with Equation (3) remains in Equation (14) for all $t \geq 0$.

$$\Omega = \left\{(S, V_1, V_2, E, I_a, I_s, R) \in R_+^7 : N(t) \leq \frac{\Lambda}{\mu}\right\}. \tag{14}$$

Hence, Ω is a positively invariant set, and on this set, the proposed model is well defined epidemiologically and mathematically. Therefore, it is sufficient to investigate the dynamics of the presented model in Ω. □

3.2. Equilibrium Points and Reproduction Number

3.2.1. Disease-Free Equilibrium Point (DFE). To calculate the DFE of Equation (2), we equate the right-hand side of Equation (2) to zero and make the disease state variables $E = I_a = I_s = 0$ and DF state variables S, V_1, V_2, and R non-zero. But at infection-free, the variables E, I_a, I_s, and R are zero. After that, solve the remaining equations of Equation (2) will give us

$$E_{\text{dfe}} = \frac{\Lambda}{(\theta + \mu)k_2k_3 - \theta(\phi_1 k_3 + \phi_2 \rho)}(k_2k_3, k_3\theta, \rho\theta, 0, 0, 0, 0). \tag{15}$$

When there is no vaccination, then Equation (15) is reduced to a fully susceptible, and it is given by

$$E_{v0} = \left(\frac{\Lambda}{\mu}, 0, 0, 0, 0, 0, 0\right). \tag{16}$$

If $\theta = 1$, then we get a DFE in which every susceptible human is vaccinated with the first dose, and

$$E_{v1} = \frac{\Lambda}{(1 + \mu)k_2k_3 - (\phi_1 k_3 + \phi_2 \rho)}(k_2k_3, k_3, \rho, 0, 0, 0, 0). \tag{17}$$

3.2.2. Basic Reproduction Number ($\mathfrak{R}_0$). The threshold quantity ($\mathfrak{R}_0$) is the average number of secondary cases produced by one primary infection during the infectious period in a fully susceptible population, and the control threshold quantity (in our case denoted by R_c) is used to represent the same quantity for a system incorporating vaccine as intervention strategies [24]. To calculate the threshold quantity, follow the work of Watmough and Driessche method. From Equation (2) and the notation $X = (E, I_a, I_s)$, we have

$$F = \begin{bmatrix} \lambda S \\ 0 \\ 0 \end{bmatrix}, \tag{18}$$

which indicates the new infection appearance at the infected state variable and

$$V = \begin{bmatrix} (\nu + \mu)E \\ (\gamma_a + \alpha_a + \mu)I_a - p\nu E \\ (\gamma_s + \alpha_s + \mu)I_s - (1-p)\nu E \end{bmatrix} = \begin{bmatrix} k_4 E \\ k_5 I_a - p\nu E \\ k_6 I_s - (1-p)\nu E \end{bmatrix} \tag{19}$$

represent the transfer of individuals into and out of the infected classes. The Jacobian matrices of F(X) and V(X) at DFE are given as blow, respectively.

$$\mathscr{F} = DF(E_{\text{dfe}}) = \frac{\mu\beta k_2 k_3}{(\theta+\mu)k_2k_3 - \theta(\phi_1 k_3 + \phi_2\rho)} \begin{bmatrix} 0 & \omega & 1 \\ 0 & 0 & 0 \\ 0 & 0 & 0 \end{bmatrix},$$

$$\mathscr{V} = DV(E_{\text{dfe}}) = \begin{bmatrix} k_4 & 0 & 0 \\ -p\nu & k_5 & 0 \\ -(1-p)\nu & 0 & k_6 \end{bmatrix}, \tag{20}$$

Now, it is simple to determine the inverse of $\mathscr{V}$ and given by

$$\mathscr{V}^{-1} = \frac{1}{k_4k_5k_6} \begin{bmatrix} k_5k_6 & p\nu k_6 & (1-p)\nu k_5 \\ 0 & k_4k_6 & 0 \\ 0 & 0 & k_4k_5 \end{bmatrix}^T. \tag{21}$$

Using the next-generation matrix,

$$\mathscr{F}\mathscr{V}^{-1} = \frac{\mu\beta k_2k_3}{k_4k_5k_6[(\theta+\mu)k_2k_3 - \theta(\phi_1k_3 + \phi_2\rho)]} \cdot \begin{bmatrix} p\nu k_6\omega + \theta(1-p)\nu k_5 & \omega k_4k_6 & k_4k_5 \\ 0 & 0 & 0 \\ 0 & 0 & 0 \end{bmatrix} \tag{22}$$

and the corresponding eigenvalues are $\lambda_1 = 0$ which is a double root and

$$\lambda_2 = \frac{\mu\beta\nu k_2k_3}{k_4k_5k_6[(\theta+\mu)k_2k_3 - \theta(\phi_1k_3 + \phi_2\rho)]}(\omega p k_6 + (1-p)k_5). \tag{23}$$

From λ_1 and λ_2, we conclude that λ_2 is the spectral radius of the next-generation matrix which equal with $\mathfrak{R}_c$ and

$$\mathfrak{R}_c = \frac{\mu\beta\nu k_2k_3}{k_4k_5k_6[(\theta+\mu)k_2k_3 - \theta(\phi_1k_3 + \phi_2\rho)]}(\omega p k_6 + (1-p)k_5). \tag{24}$$

Setting $\theta = \rho = \phi_1 = \phi_2 = 0$ in Equation (24) will give the basic reproduction number, $\mathfrak{R}_0$ as

$$\mathfrak{R}_0 = \frac{\beta\nu}{k_4k_5k_6}(\omega p k_6 + (1-p)k_5). \tag{25}$$

Now, rewriting Equation (24) in terms of $\mathfrak{R}_0$ as

$$\mathfrak{R}_c = \frac{\mu k_2k_3}{(\theta+\mu)k_2k_3 - \theta(\phi_1k_3 + \phi_2\rho)}\mathfrak{R}_0. \tag{26}$$

If $\theta = 0$, then $\mathfrak{R}_c = \mathfrak{R}_0$; otherwise, $\mathfrak{R}_c < \mathfrak{R}_0$ if $0 < \theta \leq 1$. If $\theta = 1$, then all populations are vaccinated with the first dose of vaccine. Hence, the corresponding effective (control) reproduction number is given by

$$\mathfrak{R}_1 = \frac{\mu k_2k_3}{(1+\mu)k_2k_3 - (\phi_1k_3 + \phi_2\rho)}\mathfrak{R}_0. \tag{27}$$

In general, if $\mathfrak{R}_c > 1$, then COVID-19 infections will persist in the community, and it will eventually disappear from society if $\mathfrak{R}_c < 1$.

3.2.3. Existence of Endemic Equilibrium (EE) Point of the Model. In this section, we study the disease EE of Equation (2). The main interesting idea behind the EE is that it is used to determine the existence of the disease in the human being. To find such conditions for the existence of an equilibrium for which COVID-19 is endemic in the community, at least one of $E^* \neq 0$, $I_a^* \neq 0$, or $I_s^* \neq 0$. Let us denote the steady-state solution of Equation (2) by $E_e = (S^*, V_1^*, V_2^*, E^*, I_a^*, I_s^*, R^*)$. To find E_e, equate Equation (2) to zero, and the reduced part of Equation (2) becomes

$$\begin{aligned} S^*(t) &= \frac{\Lambda k_4k_5k_6}{\beta\mu\nu(\omega p k_6 + (1-p)k_5)}, \\ V_1^*(t) &= \frac{\Lambda\theta k_4k_5k_6}{\beta\mu\nu k_2(\omega p k_6 + (1-p)k_5)}, \\ V_2^*(t) &= \frac{\Lambda\rho\theta k_4k_5k_6}{\beta\mu\nu k_2k_3(\omega p k_6 + (1-p)k_5)}, \\ E^*(t) &= \frac{\Lambda}{k_4}\left(1 - \frac{1}{\mathfrak{R}_c}\right), \\ I_a^*(t) &= \frac{\Lambda\nu p}{k_4k_5}\left(1 - \frac{1}{\mathfrak{R}_c}\right), \\ I_s^*(t) &= \frac{\Lambda\nu(1-p)}{k_4k_6}\left(1 - \frac{1}{\mathfrak{R}_c}\right), \\ R^*(t) &= \gamma_a I_a^* + \gamma_s I_s^* + \Phi V_2^*. \end{aligned} \tag{28}$$

Hence, the existence of E_e depends on $\mathfrak{R}_c$, that is, E_e of Equation (2) exists if $\mathfrak{R}_c > 1$.

3.3. Stability Analysis of Equilibrium Points. To determine the local and global asymptotic stability of the equilibria of Equation (2), we use the Jacobian matrices at DFE and EE for local stability and construct the Lyapunov function for global stability.

3.3.1. Local Stability Analyses of DFE

Theorem 3. *The disease-free-equilibrium point, E_{dfe} of Equation (2) is locally asymptotically stable (LAS) if $\mathfrak{R}_c < 1$ and unstable otherwise.*

Proof. To proof the above theorem, first calculate the Jacobian matrix of Equation (2) at E_{dfe}. That is

$$J(E_{\text{dfe}}) = \begin{bmatrix} -(\theta+\mu) & \phi_1 & \phi_2 & 0 & -\frac{\mu\beta\omega}{\Lambda}S_0 & -\frac{\mu\beta}{\Lambda}S_0 & 0 \\ \theta & -k_2 & 0 & 0 & 0 & 0 & 0 \\ 0 & \rho & -k_3 & 0 & 0 & 0 & 0 \\ 0 & 0 & 0 & -k_4 & \frac{\mu\beta\omega}{\Lambda}S_0 & \frac{\mu\beta}{\Lambda}S_0 & 0 \\ 0 & 0 & 0 & p\nu & -k_5 & 0 & 0 \\ 0 & 0 & 0 & (1-p)\nu & 0 & -k_6 & 0 \\ 0 & 0 & \Phi & 0 & \gamma_a & \gamma_s & -\mu \end{bmatrix}. \tag{29}$$

□

We now need to demonstrate that all of $J(E_{\text{dfe}})$'s eigenvalues are negative. Only the diagonal element $-\mu$ appears in the seventh column, indicating that $-\mu$ is one of the necessary eigenvalues. The remaining eigenvalues can be found in the reduced matrix, $J_1(E_{\text{dfe}})$.

$$J_1(E_{dfe}) = \begin{bmatrix} -(\theta+\mu) & \phi_1 & \phi_2 & 0 & -\frac{\mu\beta\omega}{\Lambda}S_0 & -\frac{\mu\beta}{\Lambda}S_0 \\ \theta & -k_2 & 0 & 0 & 0 & 0 \\ 0 & \rho & -k_3 & 0 & 0 & 0 \\ 0 & 0 & 0 & -k_4 & \frac{\mu\beta\omega}{\Lambda}S_0 & \frac{\mu\beta}{\Lambda}S_0 \\ 0 & 0 & 0 & p\nu & -k_5 & 0 \\ 0 & 0 & 0 & (1-p)\nu & 0 & -k_6 \end{bmatrix} \tag{30}$$

Let as assume that d_1, d_2, and d_3 are eigenvalues of M_1, and d_4, d_5, and d_6 are eigenvalues of M_2 where

$$M_1 = \begin{bmatrix} -(\theta+\mu) & \phi_1 & \phi_2 \\ \theta & -k_2 & 0 \\ 0 & \rho & -k_3 \end{bmatrix}, \qquad M_2 = \begin{bmatrix} -k_4 & \frac{\mu\beta\omega}{\Lambda}S_0 & \frac{\mu\beta}{\Lambda}S_0 \\ p\nu & -k_5 & 0 \\ (1-p)\nu & 0 & -k_6 \end{bmatrix}. \tag{31}$$

The characteristic equation of M_1 is

$$d^3 + b_1 d^2 + b_2 d + b_3 = 0, \tag{32}$$

where

$$\begin{aligned} b_1 &= k_2 + k_3 + (\theta+\mu), \\ b_2 &= k_2k_3 + k_3(\theta+\mu) + k_2(\theta+\mu) - \phi_1\theta k_3, \\ b_3 &= k_2k_3(\theta+\mu) - \phi_1\theta k_3 - \phi_2\theta\rho. \end{aligned} \tag{33}$$

Clearly, we see that $b_1 > 0$ and $b_2 > 0$ because they are the sum of positive parameters. But from the third equation, i.e.,

$$\begin{aligned} b_3 &= k_2k_3(\theta+\mu) - \phi_1\theta k_3 - \phi_2\theta\rho, \\ b_3 &= b_3 - \frac{\mu\beta\nu k_2k_3}{k_4k_5k_6}(\omega p k_6 + (1-p)k_5) + \frac{\mu\beta\nu k_2k_3}{k_4k_5k_6}(\omega p k_6 + (1-p)k_5), \\ b_3 &= \frac{\mu\beta\nu k_2k_3}{k_4k_5k_6}(\omega p k_6 + (1-p)k_5) + b_3\left(1 - \frac{\mu\beta\nu k_2k_3}{k_4k_5k_6b_3}(\omega p k_6 + (1-p)k_5)\right), \\ b_3 &= \frac{\mu\beta\nu k_2k_3}{k_4k_5k_6}(\omega p k_6 + (1-p)k_5) + b_3(1-\mathfrak{R}_c). \end{aligned} \tag{34}$$

We also say that $b_3 > 0$ if and only if $\mathfrak{R}_c < 1$. In the same fashion, the characteristic equation of M_2 is

$$d^3 + b_4 d^2 + b_5 d + b_6 = 0. \tag{35}$$

where

$$\begin{aligned} b_4 &= k_4 + k_5 + k_6, \\ b_5 &= k_4k_5 + k_4k_6 + k_5k_6 - \frac{\mu\beta\nu k_2k_3}{(\theta+\mu)k_2k_3 - \theta(\phi_1k_3 + \phi_2\rho)}(\omega p + (1-p)), \\ b_6 &= k_4k_5k_6 - \frac{\mu\beta\nu k_2k_3}{(\theta+\mu)k_2k_3 - \theta(\phi_1k_3 + \phi_2\rho)}(\omega p k_6 + (1-p)k_5), \\ b_6 &= k_4k_5k_6\left(1 - \frac{\mu\beta\nu k_2k_3}{k_4k_5k_6((\theta+\mu)k_2k_3 - \theta(\phi_1k_3 + \phi_2\rho))}(\omega p k_6 + (1-p)k_5)\right), \\ b_6 &= k_4k_5k_6(1-\mathfrak{R}_c). \end{aligned} \tag{36}$$

Since b_4 and b_5 of Equation (35) are greater than zero because they are the sum of positive parameters, and $b_6 > 0$

if and only if $\mathfrak{R}_c < 1$. To check the negativity of the eigenvalues, we used the Routh-Hurwitz criteria and by this principle Equation (32) has a strictly negative real root if and only if $b_1 > 0$, $b_2 > 0$, and $b_3 > 0$ and Equation (35) has strictly negative real root if and only if $b_4 > 0$, $b_5 > 0$, and $b_6 > 0$. Therefore, we conclude that E_{dfe} of system Equation (2) is LAS if $\mathfrak{R}_c < 1$ and unstable otherwise.

Theorem 4. *The disease-endemic equilibrium point (E_e) of the model on Equation (2) above is locally asymptotically stable (LAS) in Ω if $\mathfrak{R}_c > 1$ and unstable if $\mathfrak{R}_c < 1$.*

The proof is as straight-forward as [25].

3.3.2. Global Stability Analyses of DFE

Theorem 5. *The disease-free equilibrium point of the dynamical system on Equation (2) is globally asymptotically stable (GAS) if $\mathfrak{R}_c < 1$ and unstable otherwise.*

Proof. To proof global stability of E_{def}, we first construct the Lyapunov function [25]. Let the Lyapunov function be $V : R_+^7 \longrightarrow R_+$ and defined as

$$V(S, V_1, V_2, E, I_a, I_s, R) = a_1 S + a_2 E + a_3 I_a + a_4 I_s, \tag{37}$$

$$\frac{dV}{dt} = a_1 \frac{dS}{dt} + a_2 \frac{dE}{dt} + a_3 \frac{dI_a}{dt} + a_4 \frac{dI_s}{dt}, \tag{38}$$

$$\begin{aligned} \frac{dV}{dt} = {} & a_1(\Lambda + \phi_1 V_1 + \phi_2 V_2 - (\theta + \lambda + \mu)S) \\ & + a_2(\lambda S - (\mu + \nu)E) + a_3(p\nu E - (\mu + \gamma_a + \alpha_a)I_a) \\ & + a_4((1-p)\nu E - (\mu + \gamma_s + \alpha_s)I_s). \end{aligned} \tag{39}$$

□

To determine constants, equate the partial derivatives of Equation (37) with respect to S, E, I_a, and I_s to zero. Hence, to determine a_1, equate the partial derivatives of Equation (37) in terms of S to zero, and we will obtain

$$-a_1(\theta + \mu) = 0 \Longrightarrow a_1 = 0. \tag{40}$$

Partial derivative in terms of E gives us $-a_2 k_4 + a_3 p\nu + a_4((1-p)\nu) = 0$, and from this we obtain

$$a_2 = \frac{(\mathrm{a}_3 p\nu + a_4(1-p)\nu)}{k_4}. \tag{41}$$

Partial derivative in terms of I_a gives us $-a_1\beta\omega(S^0/N) + a_2\beta\omega(S^0/N) - a_3 k_5 = 0$, and this gives us

$$a_3 = -\frac{(a_1 - a_2)}{k_5}\beta\omega\frac{S^0}{N}. \tag{42}$$

Partial derivative in terms of I_s gives us $-a_1\beta(S^0/N) + a_2\beta(S^0/N) - a_4 k_6 = 0$, and from this gives

$$a_4 = -\frac{(a_1 - a_2)}{k_6}\beta\frac{S^0}{N}. \tag{43}$$

Since $S \le S^0$, and substituting a_1, a_2, a_3, and a_4 into Equation (37) and after some simplification

$$\begin{aligned} \frac{dV}{dt} &= a_2\left(\frac{\beta\nu S^0}{N k_5 k_6}(k_6\omega p + k_5(1-p)) - k_4\right)E, \\ \frac{dV}{dt} &= a_2 k_4(\mathfrak{R}_v - 1)E. \end{aligned} \tag{44}$$

Since $a_2 k_4 \ge 0$, then $dV/dt = a_2 k_4(\mathfrak{R}_c - 1) \le 0$ where $\mathfrak{R}_c \le 1$ and $dV/dt = 0$ if and only if $S = E = I_a = I_s = 0$. This implies that the only trajectory of Equation (2) on which $dV/dt \le 0$ is E_{dfe}. Hence, by LaSalle's invariance principle, the E_{dfe} is GAS in Ω if $\mathfrak{R}_c \le 1$; otherwise, it is unstable.

3.3.3. Global Stability Analyses of EEP

Theorem 6. *If $\mathfrak{R}_c > 1$, then the disease EEP (E_e) of Equation (2) is GAS in Ω.*

Proof. Since diseases EEP exist for $\mathfrak{R}_c > 1$, then to prove the GAS behavior of E_e, we apply [26, 27] approach as

$$L = \sum_1^n \left(x_i - x_i^* - x_i^* \ln\left(\frac{x_i}{x_i^*}\right)\right), \tag{45}$$

where x_i is a state variable, $i = 1,\ldots 7$ and x_i^* is the endemic equilibrium point. From Equation (45), we have

$$\begin{aligned} L(S^*, V_1^*, V_2^*, E^*, I_a^*, I_a^*, R^*) = {} & \left(S - S^* - S^* \ln\left(\frac{S}{S^*}\right)\right) \\ & + \left(V_1 - V_1^* - V_1^* \ln\left(\frac{V_1}{V_1^*}\right)\right) + \left(V_2 - V_2^* - V_2^* \ln\left(\frac{V_2}{V_2^*}\right)\right) \\ & + \left(E - E^* - E^* \ln\left(\frac{E}{E^*}\right)\right) + \left(I_a - I_a^* - I_a^* \ln\left(\frac{I_a}{I_a^*}\right)\right) \\ & + \left(I_s - I_s^* - I_s^* \ln\left(\frac{I_s}{I_s^*}\right)\right) + \left(R - R^* - R^* \ln\left(\frac{R}{R^*}\right)\right). \end{aligned} \tag{46}$$

□

Having derivative of Equation (45) in the direction of the solution of Equation (2) and replacing dS/dt, dV_1/dt, dV_2/dt, dE/dt, dI_a/dt, dI_s/dt, and dR/dt by their respective expression from Equation (2), we get

$$\frac{dL}{dt} = \left(1 - \frac{S^*}{S}\right)\left(\Lambda + \phi_1 V_1 + \phi_2 V_2 - \left(\theta + \beta\frac{(\omega I_a + I_s)}{N} + \mu\right)S\right) + \left(1 - \frac{V_1^*}{V_1}\right)(\theta S - k_2 V_1) + \left(1 - \frac{V_2^*}{V_2}\right)(\rho V_1 - k_3 V_2) + \left(1 - \frac{E^*}{E}\right)\left(\beta\frac{(\omega I_a + I_s)}{N}S - k_4 E\right) + \left(1 - \frac{I_a^*}{I_a}\right)(p\nu E - k_5 I_a) + \left(1 - \frac{I_s^*}{I_s}\right)((1-p)\nu E - k_6 I_s) + \left(1 - \frac{R^*}{R}\right)(\gamma_a I_a + \gamma_s I_s + \Phi V_2 - \mu R). \tag{47}$$

Expanding the above equation will give us

$$\frac{dL}{dt} = \Lambda + \phi_1 V_1 + \phi_2 V_2 - \mu S - \Lambda\frac{S^*}{S} - \phi_1 V_1\frac{S^*}{S} - \phi_2 V_2\frac{S^*}{S} + \mu S^* + \beta\frac{(\omega I_a + I_s)}{N}S^* + \theta S^* - k_2 V_1 - \theta S\frac{V_1^*}{V_1} + \rho V_1 - k_3 V_2 - \rho V_1\frac{V_2^*}{V_2} + k_3 V_2^* - k_4 E - \beta\frac{(\omega I_a + I_s)}{N}S\frac{E^*}{E} + k_4 E^* - k_5 I_a - p\nu E\frac{I_a^*}{I_a} + k_5 I_a^* + \nu E - k_6 I_s - (1-p)\nu E\frac{I_s^*}{I_s} + k_6 I_s^* + \gamma_a I_a + \gamma_s I_s + \Phi V_2 - \mu R - \gamma_a I_a\frac{R^*}{R} - \gamma_s I_s\frac{R^*}{R} - \Phi V_2\frac{R^*}{R} - \mu R^*. \tag{48}$$

Further simplification result to

$$\frac{dL}{dt} = \Lambda + \phi_1 V_1 + \phi_2 V_2 + \left(\theta + \mu + \beta\frac{(\omega I_a + I_s)}{N}\right)S^* + \rho V_1 + k_3 V_2^8 + k_4 E^* + k_5 I_a^* + \nu E + k_6 I_s^* + \gamma_a I_a + \gamma_s I_s + \Phi V_2 + \mu R^* - \left(\left(\mu + \theta\frac{V_1^*}{V_1} + \beta\frac{(\omega I_a + I_s)}{N}\right)S^* + (\Lambda + \phi_1 V_1 + \phi_2 V_2)\frac{S^*}{S} + \right) - \left(\left(k_2 + \rho\frac{V^*}{V_2}\right)V_1 + k_4 E + k_5 I_a + k_6 I_s + p\nu E\frac{I_a^*}{I_a} + (1-p)\nu E\frac{I_s^*}{I_s} + (\gamma_a I_a + \gamma_s I_s + \Phi V_2)\frac{R^*}{R}\right). \tag{49}$$

Now, we can write dL/dt as $dL/dt = \Psi_1 - \Psi_2$, where

$$\Psi_1 = \Lambda + \phi_1 V_1 + \phi_2 V_2 + \left(\theta + \mu + \beta\frac{(\omega I_a + I_s)}{N}\right)S^* + \rho V_1 + k_3 V_2^8 + k_4 E^* + k_5 I_a^* + \nu E + k_6 I_s^* + \gamma_a I_a + \gamma_s I_s + \Phi V_2 + \mu R^*,$$

$$\Psi_2 = \left(\mu + \theta\frac{V_1^*}{V_1} + \beta\frac{(\omega I_a + I_s)}{N}\right)S^* + (\Lambda + \phi_1 V_1 + \phi_2 V_2)\frac{S^*}{S} + \left(k_2 + \rho\frac{V^*}{V_2}\right)V_1 + k_4 E + k_5 I_a + k_6 I_s + p\nu E\frac{I_a^*}{I_a} + (1-p)\nu E\frac{I_s^*}{I_s} + (\gamma_a I_a + \gamma_s I_s + \Phi V_2)\frac{R^*}{R}. \tag{50}$$

From the fact that all the parameter values considered in Equation (2) are positive, hence $dL/dt \le 0$ if $\Psi_1 \le \Psi_2$ and $dL/dt = 0$ if and only if $\Psi_1 = \Psi_2$ which mean $dL/dt = 0 \Leftarrow S = S^*,\ V_1 = V_1^*,\ V_2 = V_2^*,\ E = E^*,\ I_a = I_a^*,\ I_s = I_s^*$, and $R = R^*$. Thus, by LaSalle's invariance principle, the E_e is GAS in Ω if $\Psi_1 < \Psi_2$.

4. Estimation of the parameter's Value

In this manuscript, we solve a dynamics of parameter estimation problem via a daily-wise reported number of coronavirus confirmed cases in Ethiopia from July 1, 2022, to August 31, 2022, see Table 2. The best fit corresponding to the daily-wise reported confirmed individuals via our model is shown in Figure 2 using the MATLAB routine. Here, we fitted some number of the model parameter's value such as p, ω, θ, ρ, ϕ_1, ϕ_2, and Φ, whereas the remaining parameter's value was taken from well-published literature or estimated, see Table 1. Furthermore, the initial conditions of the presented model are estimated according to the demographic data of Ethiopia and the real reported COVID-19 patient by the Ethiopian Ministry of Health 2022 and Ethiopian World in Data (Our World in Data, COVID-19 2022) between July 01, 2022, and August 31, 2022 [28]. The calculated parameters from the reported data in Ethiopia are estimated as follows: The total population size of Ethiopia in 2022 is approximately $N = 110,000,000$ during the specified days, and the life expectancy of Ethiopians for the year 2022 is 67.8 [23]. And the natural death rate (μ) is calculated as $\mu = 1/(365 * 67.8)$, while $\Lambda = \mu * N(0)$. According to the Ethiopian Federal Ministry of Health report, there have been 281 active COVID-19 cases, i.e., $I_s(0) = 281$, and from the WHO report, 80% of infected humans become asymptomatic; hence, we estimated I_a as $I_a(0) = 281/0.8$. We let $E(0) = 650$, which is approximately equivalent to the sum of I_a and I_s [20]. Consequently, assuming $V_1(0)$=500, $V_2(0)$=300, $R(0) = 200$, and $N(0) = 3002282$ then $S(0)$ is estimated as $S(0) = N(0) - (V_1(0) + V_2(0) + E(0) + I_a(0) + I_s(0) + R(0))$.

The fitted parameter's values are demonstrated using the least-squares method to minimize the summation of squared errors defined on Equation (53). The system of Equation (2) is formulated as a standard dynamic system in the following form:

$$y' = f(t, y, p), \tag{51}$$

$$y(t_0) = y_0, \tag{52}$$

Table 2: Daily COVID-19 confirmed reports in Ethiopia, from July 1, 2022, to August 31, 2022 [28].

Days	Infected	Days	Infected	Days	Infected	Days	Infected
1	281	17	55	33	38	48	26
2	250	18	0	34	59	49	20
3	86	19	199	35	37	50	41
4	161	20	124	36	49	51	25
5	154	21	99	37	15	52	8
6	190	22	134	38	15	53	42
7	185	23	87	39	58	54	22
8	151	24	30	40	41	55	44
9	114	25	75	41	41	56	13
10	74	26	83	42	36	57	43
11	116	27	62	43	46	58	10
12	71	28	67	44	25	59	2
13	138	29	79	45	15	60	23
14	121	30	69	46	63	61	13
15	109	31	43	47	32	62	10
16	106	32	41				

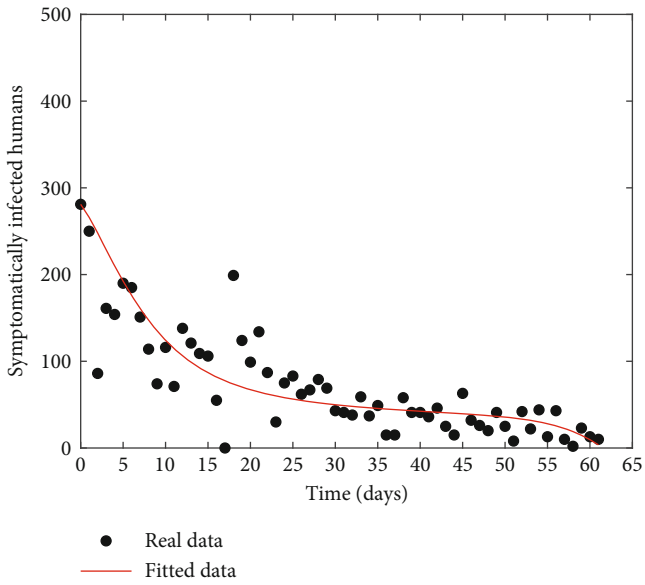

Figure 2: Daily time series of COVID-19 data from July 1 to August 31, 2022.

where y represent vector of the dependent variables (compartments) and p is the vector of unknown parameters. The associated sum-of-square error is given by

$$\varphi = \sum_{i=1} (y_i - \bar{y}_i)^2, \tag{53}$$

where y_i stands for the real data and $y_i = y(t_i, p)$ is the solution of Equation (51) with initial condition Equation (52) according to the number of infected individuals at time t_i for a given set of estimated parameters p. The main goal is to minimize the objective function

$$\min_p \varphi(p), \tag{54}$$

subject to Equation (53) to obtain the required fitted parameter values [29].

4.1. Estimation of Basic Reproduction Number ($\mathfrak{R}_c$). The basic reproduction number of any disease shows how fast the disease can spread throughout susceptible populations. In this case, we have a control reproduction parameter, $\mathfrak{R}_c$, in the presence of a vaccine and a simple reproduction number $\mathfrak{R}_0$ in the absence of a vaccine in our model. Particularly, if $\mathfrak{R}_c > 1$, then the disease can spread into the susceptible population, and if $\mathfrak{R}_c < 1$, then the disease dies out from the community. So in this section, we estimate the numerical value of $\mathfrak{R}_c$ for Equation (2). Substituting the corresponding parameter's value in Equation (25) and Equation (26) from Table 1, we get the following estimated results. $\mathfrak{R}_0 = 2.105062463$, $\mathfrak{R}_c = 0.0007495074407$, and $\mathfrak{R}_1 = 0.00008555327934$. Therefore, the value of $\mathfrak{R}_0$ is approximately 2.11 which indicates 2 or 3 susceptible individuals can be infected by a single infected human because of no vaccination and any other control mechanisms in the model. Similarly, $\mathfrak{R}_c$ is approximately 0.001 indicates that the diseases cannot spread into the population due to the presence of control strategies in the model like vaccination.

5. Sensitivity Analysis

In this section, we carried out a sensitivity analysis of the parameters in the basic reproduction number to identify their impact on the transition dynamics of the COVID-19 pandemic. To go through this section, we used the normalized sensitivity index definition as stated in [30]. The Normalized forward sensitivity index of a variable, $\mathfrak{R}_c$, that

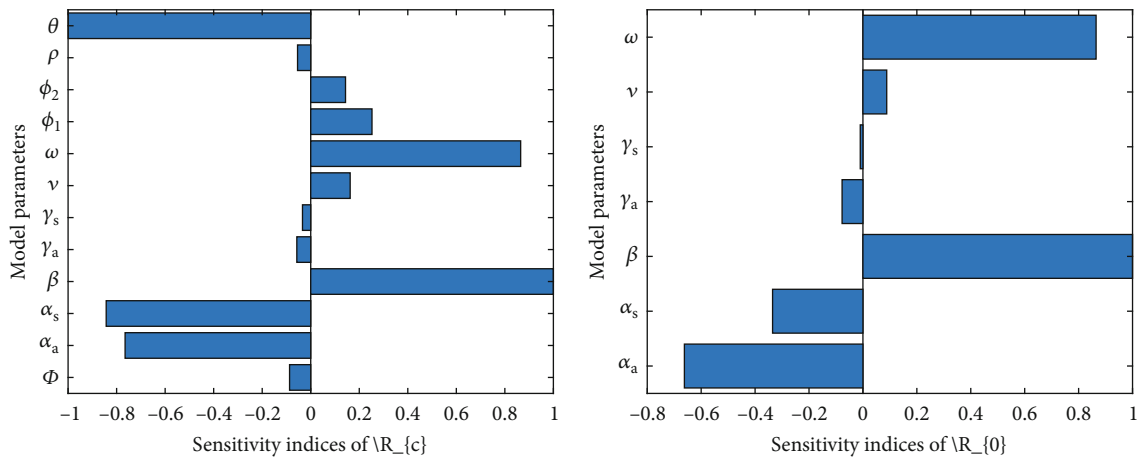

Figure 3: Correlation between the $\mathfrak{R}_0$ and $\mathfrak{R}_c$ and the model parameters β, ν, α_a, α_s, γ_a, γ_s, ω, θ, ρ, Φ, ϕ_1, and ϕ_2.

depends on the differentiability of $\mathfrak{R}_c$ with respect to a parameter, φ, is defined as

$$\Lambda_{\varphi}^{\mathfrak{R}_c} = \frac{\partial \mathfrak{R}_c}{\partial \varphi}\frac{\varphi}{\mathfrak{R}_c}. \tag{55}$$

For φ represents all the parameters in $\mathfrak{R}_c$

$$\begin{aligned}
&\text{For } \varphi = \nu, \Lambda_{\nu}^{(\mathfrak{R}_0)} = \frac{(\partial \mathfrak{R}_c)}{\partial \nu}\frac{\nu}{\mathfrak{R}_c} = 1 - \frac{\nu}{k_4} > 0,\\
&\text{For } \varphi = \omega, \Lambda_{\omega}^{\mathfrak{R}_c} = \frac{\partial \mathfrak{R}_c}{\partial \omega}\frac{\omega}{\mathfrak{R}_c} = \frac{\omega p k_6}{\omega p k_6 + (1-p)k_5} > 0,\\
&\text{For } \varphi = \theta, \Lambda_{\theta}^{\mathfrak{R}_c} = \frac{\partial \mathfrak{R}_c}{\partial \theta}\frac{\theta}{\mathfrak{R}_c} = -\theta\frac{(k_2k_3 - (\phi_1k_3 + \phi_2\rho))}{(\theta+\mu)k_2k_3 - \theta(\phi_1k_3 + \phi_2\rho)} < 0.
\end{aligned} \tag{56}$$

The same method can be used to determine the index values of the other parameters. And as depicted in Figure 3, the parameters (β, ω, ν, ϕ_1, and ϕ_2) have positive indices. This shows us they have a great impact on the spreading of the disease in the community; as their values increase the disease expands through the population, and as their values decrease, the diseases become eliminated from the population. In addition, the parameters in which their sensitivity indices are negative (θ, α_a, α_s, γ_1, γ_1, Φ, and ρ) have an effect of reducing the burden of the disease in the population as their values increase. Therefore, research advice for stakeholders is to work on minimizing the positive indices and maximizing the negative indices of the parameters.

6. Optimal Control Analysis

In this section, we examine the following two suggested control methods, which are crucial in reducing the dynamics of the new coronavirus epidemic transmission. Thus, $c_1(t)$ and $c_2(t)$, which stand for the following terms, are used to signify time-dependent control variables:

(i) The preventive measures focused on inhibiting the transmission dynamics of the virus from symptomatic and asymptomatic humans. This can be obeyed through public health advocacy for wearing face masks in public places, regular hand washing, social distancing, quarantine, and isolation that help reduce the contact rate. Noting that $c_1(t) = 1$ implies the strategy is effective for protection against infection, while $c_1(t) = 0$ implies failure of the strategy

(ii) The treatment measure includes medical care for all the confirmed cases to increase the recovery rate of infected individuals and to decrease disease-induced mortality rate. This can be achieved by rapidly giving patients who are hospitalized with COVID-19 a critical case of additional oxygen or mechanical breathing

Consequently, by including these control variables in Equation (2), we obtain

$$\begin{cases}
\dfrac{dS}{dt} = \Lambda + \phi_1V_1 + \phi_2V_2 - (1-c_1)\beta\dfrac{(\omega I_a + I_s)}{N}S - (\theta+\mu)S,\\
\dfrac{dV_1}{dt} = \theta S - (\mu + \rho + \phi_1)V_1,\\
\dfrac{dV_2}{dt} = \rho V_1 - (\mu + \phi_2 + \Phi)V_2,\\
\dfrac{dE}{dt} = (1-c_1)\beta\dfrac{(\omega I_a + I_s)}{N}S - (\mu+\nu)E,\\
\dfrac{dI_a}{dt} = p\nu E - (\mu + \gamma_a + \alpha_a + c_2)I_a,\\
\dfrac{dI_s}{dt} = (1-p)\nu E - (\mu + \gamma_s + \alpha_s + c_2)I_s,\\
\dfrac{dR}{dt} = (\gamma_a + c_2)I_a + (\gamma_s + c_2)I_s + \Phi V_2 - \mu R.
\end{cases} \tag{57}$$

The primary task at hand is to identify the best possible control for preventive measures c_1 and c_2, given the relatively low costs of these techniques. The Pontryagin maximum principle [31] is used to establish the necessary and sufficient conditions for the existence of optimal control. The function that minimizes the number of exposed cases and symptomatically and asymptomatically infected cases over a time interval of $[0, t_f]$ can be defined as

$$J_{\text{op}}(c_1, c_2) = \min_{0 \le c_1, c_2 \le 1} \int_0^{t_f} \left(b_1 E + b_2 I_a + b_3 I_s + \frac{1}{2} \sum_{i=1}^{2} w_i c_i^2 \right) dt \tag{58}$$

subject to Equation (57) with associated initial conditions defined on Equation (3). The positive constants b_1, b_2, and b_3 are used to balance the units of the integrand to reduce the dominance of any one of the terms in the integral, and w_1 and w_2 measure the relative cost of intervention strategies over the time interval $[0, t_f]$. Minimizing Equation (58) provides an optimal control $c_i^* = 1, 2$ such that

$$J_{op}(c_1^*, c_2^*) = \min \left\{ J_{op} \frac{c_1, c_2}{c_i} \in C \right\}, \tag{59}$$

subject to the control-induced state Equation (57) with prescribed initial data and where $C = (c_1, c_2)$: each c_i is measurable with $0 \le c_i < 1$, $i = 1, 2$ for $t \in [0, t_f]$. The solution of Equation (57) or the optimal control problem is the vector function $(S^*, V_1^*, V_2^*, E, I_a^*, I_s^*, R^*) \in R_+^7$ associated with an optimal control pair $(c_1^*, c_2^*) \in C$ on the time interval $[0, t_f]$ that minimizes the cost functional Equation (58).

6.1. Characterization of Optimal Control. In this part, we outline the features of the optimum control problem defined in Equation (57) and offer the optimality requirements. According to Pontryagin's maximum principle [32], if (c_1^*, c_2^*) is optimal for problem Equation (57) with the associated initial condition given in Equation (3) and Equation (58) with fixed final time t_f, then there exists a non-trivial absolutely continuous mapping $\lambda : [0, t_t] \longrightarrow R^7$, $\lambda = (\lambda_1(t), \lambda_2(t), \lambda_3(t), \lambda_4(t), \lambda_5(t), \lambda_6(t), \lambda_7(t))$ called the adjoint vector, such that

(1) The Hamiltonian function is defined as

$$\begin{aligned} H = {} & b_1 E + b_2 I_a + b_3 I_s + \frac{1}{2} \sum_{i=1}^{2} w_i c_i^2 \\ & + \sum_{i=1}^{7} \lambda_i(t) g_i(t, S, V_1, V_2, E, I_a, I_s, R, c), \end{aligned} \tag{60}$$

where g_i represents the right hands of Equation (57) for $i = 1, 2, 3, 4, 5, 6, 7$.

(2) The optimal condition of the system

$$\frac{\partial H}{\partial c_i} = 0, i = 1, 2. \tag{61}$$

Moreover, from Equation (61) the corresponding optimal controls c_1^* and c_2^* are given by

$$c_1^* = \max \left\{ 0, \min \left\{ 1, (\lambda_4 - \lambda_1) \mu \beta \frac{(\omega I_a + I_s)}{\Lambda w_1} S^* \right\} \right\}, \tag{62}$$

$$c_2^* = \max \left\{ 0, \min \left\{ 1, \frac{(\lambda_5 - \lambda_7) I_a^* + (\lambda_6 - \lambda_7) I_s^*}{w_2} \right\} \right\}. \tag{63}$$

(3) Hamiltonian system which is the combination of the control system and the adjoint system, respectively, defined in

$$\begin{aligned} S' &= \frac{\partial H}{\partial \lambda_1}, \\ V_1' &= \frac{\partial H}{\partial \lambda_2}, \\ V_2' &= \frac{\partial H}{\partial \lambda_3}, \\ E' &= \frac{\partial H}{\partial \lambda_4}, \\ I_a' &= \frac{\partial H}{\partial \lambda_5}, \\ I_s' &= \frac{\partial H}{\partial \lambda_6}, \\ R' &= \frac{\partial H}{\partial \lambda_7}, \\ \lambda_1' &= -\frac{\partial H}{\partial S}, \\ \lambda_2' &= \frac{\partial H}{\partial V_1}, \\ \lambda_3' &= \frac{\partial H}{\partial V_2}, \\ \lambda_4' &= \frac{\partial H}{\partial E}, \\ \lambda_5' &= \frac{\partial H}{\partial I_a^*}, \\ \lambda_6' &= \frac{\partial H}{\partial I_s}, \\ \lambda'_7 &= \frac{\partial H}{\partial R}. \end{aligned} \tag{64}$$

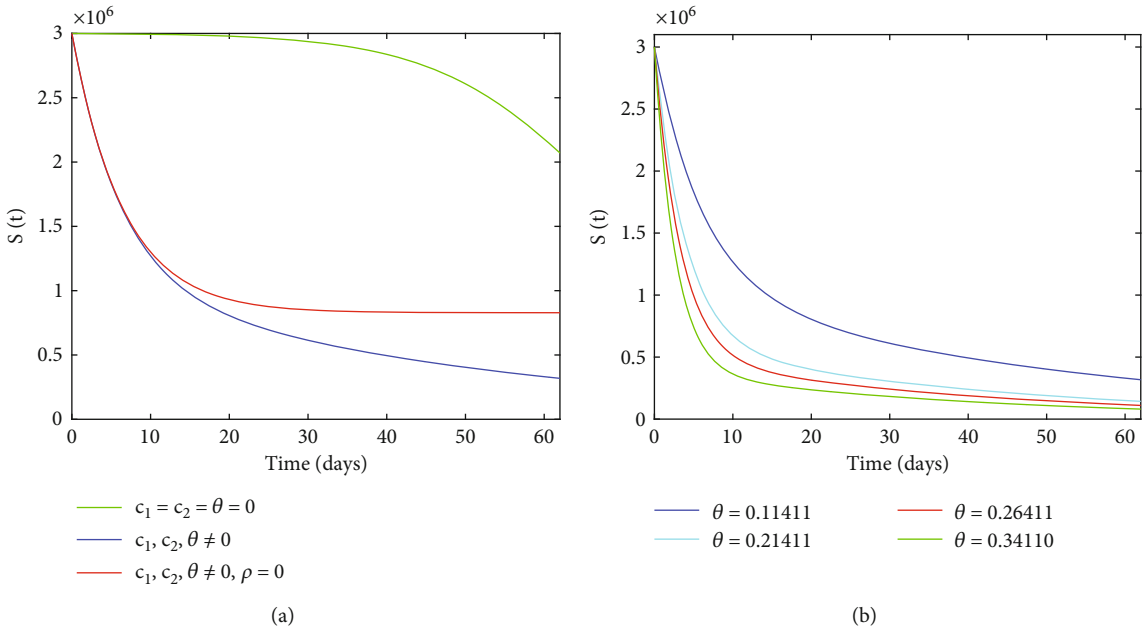

Figure 4: Impact of vaccine and control variables on susceptible humans.

(4) The transversality condition of the model is also holds true. That is

$$\lambda_i(t_f) = 0, \quad i = 1, 2, 3, 4, 5, 6, 7. \tag{65}$$

Next, we discuss the characterization of optimal controls and adjoint variables.

Theorem 7 (Necessary optimality conditions). *Suppose* (c_1^*, c_2^*) *is the optimal control and* $(S^*, V_1^*, V_2^*, E^*, I_a^*, I_s^*,$ *and* $R^*)$ *is the corresponding unique optimal solution of the optimal control problem given in Equation (57) with the initial condition defined in Equation (3) and Equations (60) and (61) with a fixed final time* t_f. *Then there exists an adjoint function* $\lambda_i^*(t), i = 1, 2, 3, 4, 5, 6, 7$ *satisfying the following adjoint system:*

$$\begin{cases} \frac{d\lambda_1}{dt} = (\lambda_1 - \lambda_4 - b_1)(1 - c_1)\beta\mu\frac{(\omega I_a + I_s)}{\Lambda} + (\theta + \mu)\lambda_1 - \theta\lambda_2, \\ \frac{d\lambda_2}{dt} = (\lambda_2 - \lambda_1)\phi_1 + (\lambda_2 - \lambda_3)\rho + \mu\lambda_2, \\ \frac{d\lambda_3}{dt} = (\lambda_3 - \lambda_1)\phi_2 + (\lambda_3 - \lambda_7)\Phi + \mu\lambda_3, \\ \frac{d\lambda_4}{dt} = (b_1 + \lambda_4)(\mu + \nu) + (\lambda_6 - \lambda_5 - b_2 + b_3)p\nu - (b_3 + \lambda_6)\nu, \\ \frac{d\lambda_5}{dt} = (\lambda_1 - \lambda_4 - b_1)(1 - c_1)\frac{\beta\omega\mu}{\Lambda}S + (\lambda_5 + b_2)(\mu + \gamma_a + \alpha_a + c_2) - \lambda_7(\gamma_a + c_2), \\ \frac{d\lambda_6}{dt} = (\lambda_1 - \lambda_4 - b_1)(1 - c_1)\frac{\beta\mu}{\Lambda}S + (b_3 + \lambda_6)(\mu + \gamma_s + \alpha_s + c_2) - \lambda_7(\gamma_s + c_2), \\ \frac{d\lambda_7}{dt} = \mu\lambda_7. \end{cases} \tag{66}$$

subject to transiversality conditions defined on Equation (65).

Proof. The adjoint equations, optimality condition, and transversality conditions can be obtained via Pontryagin's maximum principle [33]. Thus, system, conditions, and equations are derived as above. That is Equation (66) from Equation (64), Equation (62), and Equation (63) from Equation (61). This completes the proof. □

7. Numerical Simulations and Its Discussion

In order to validate the analytical findings mentioned in Section 3, numerical simulations of the model utilizing the MATLAB programming language's ordinary differential equation solvers are presented in this section. Furthermore, we may statistically observe how control measures affect the coronavirus outbreak's spread in the model outlined in Section 6. To illustrate the numerical results, use the initial conditions defined in Section 4 and the parameters in Table 1.

To determine the optimal solution of the optimality system, an iterative scheme is used. Since our aim is to control the diseases, the numerical simulations carried out on the control system Equation (57), adjoint equations defined on Equation (64) with respect to Equation (65) and characterizations of the control defined on Equation (62) and Equation (63) are run in MATLAB using the Runge-Kutta forward-backward sweep method to support the analytical results discussed in Sections 3 and 6.

An iterative scheme is used to find the optimal solution to the optimality system. Since the state Equation (2) has initial conditions and the adjoint systems (66) have final conditions, we solve the state system using a forward fourth-order Runge–Kutta method and solve the adjoint system using a backward fourth-order Runge–Kutta method. The iterative solution scheme involves making a guess of the controls and using that guess to solve the state system. The initial guess of the control together with the solution

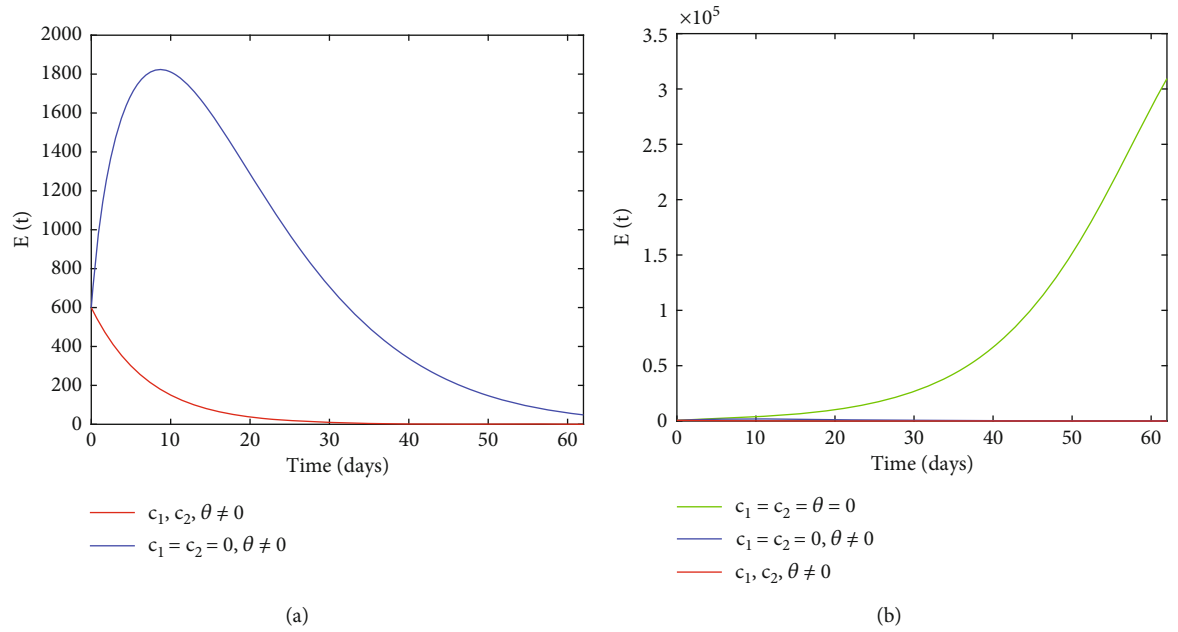

Figure 5: Impact of vaccine and control variables on exposed humans.

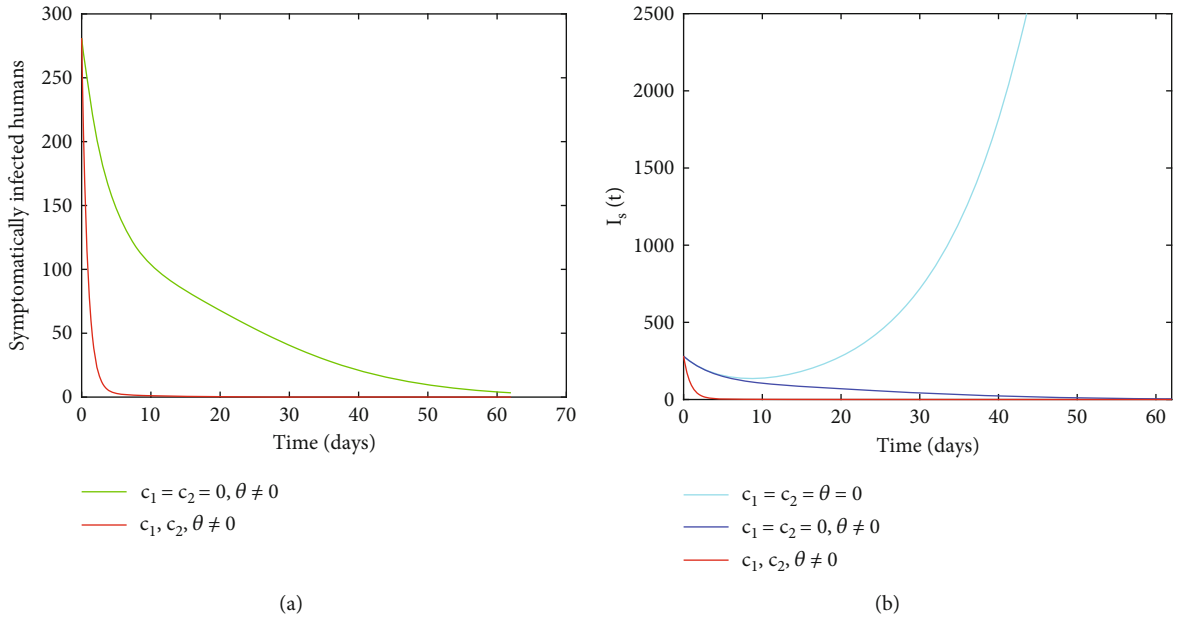

Figure 6: Impact of vaccine and control variables on symptomatically infected humans.

of the state systems is used to solve the adjoint systems. The controls are then updated using a convex combination of the previous controls and the values obtained using the characterizations. The solution of the state and adjoint systems is then repeated using the updated controls. This process is repeated until the values in the current iteration are close enough to the previous iteration values.

The impact of first- and second-dose vaccines, prevention, and treatment control strategies on susceptible, exposed, infected, and recovered humans is discussed qualitatively below.

7.1. Impact of Full Dose Vaccine and Prevention on S(T). Figure 4 illustrates the impact of full-dose vaccination on the susceptible population. In Figure 4(a), the blue line depicts the effect of a full dose booster on susceptible humans, that is, (ρ) and (θ), while the red line indicates the significant impact of a second shot of COVID-19 vaccine. The green line shows the absence of both dose vaccination, prevention, and treatment on susceptible individuals. Simply Looking at the figure, we can conclude that full doses of vaccines have a more significant impact on reducing the risk of susceptible humans. Figure 4(b) illustrates the

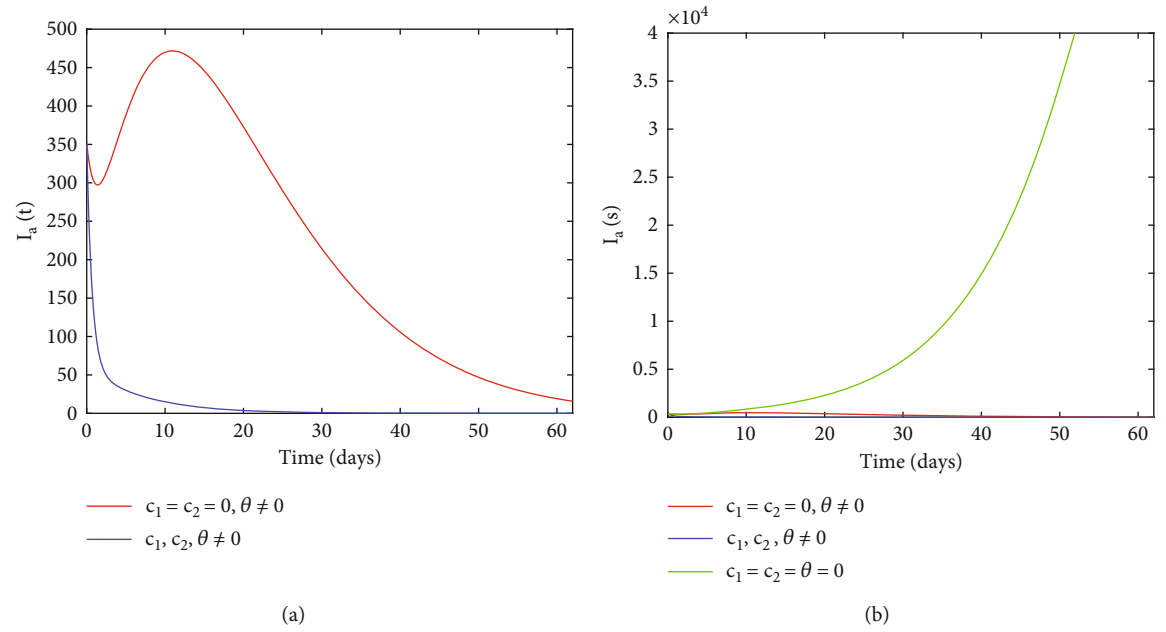

FIGURE 7: Impact of vaccine and control variables on asymptomatically infected humans.

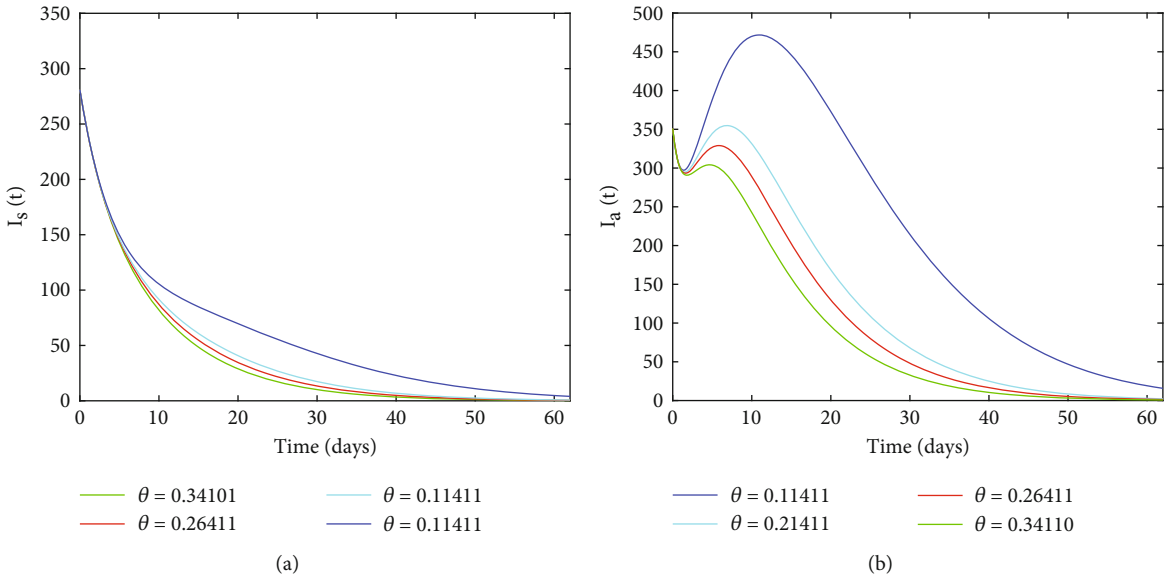

FIGURE 8: Impact of the first dose vaccine on symptomatically and asymptomatically infected humans.

influence of the first dose vaccination rate (θ) on susceptible individuals. Also, we observed that the susceptibility of individuals to COVID-19 can be decreased significantly when we increase the first-shot vaccination rate sufficiently. It is visible from Figure 4 that taking full-dose vaccination in parallel with prevention and treatment control strategies decreases the susceptibility of individuals to the COVID-19 virus. From a biological view, when the second dose vaccination rate Φ increases, it provides humans with herd immunity against the virus.

7.2. Impact Control Strategies on E(T). The blue solid line in Figure 5(a) depicts the proportion of exposed people who received vaccinations but did not use any additional preventative measures. It rises initially before progressively falling off after 15 days. But when we use vaccinations and control strategies simultaneously, as shown in Figure 5(a), with a red solid line from the beginning, the exposed cases decrease rapidly until there are no exposed humans as time increases. This depicts how the use of both doses of vaccination, prevention, and treatments at the same time can eliminate the risk of an outbreak of the diseases. From Figure 5(b), we can conclude that if there are no control strategies, then the exposed cases increase with time. From a biological explanation, when there is no vaccination and other control strategies, anybody can be easily exposed to the disease.

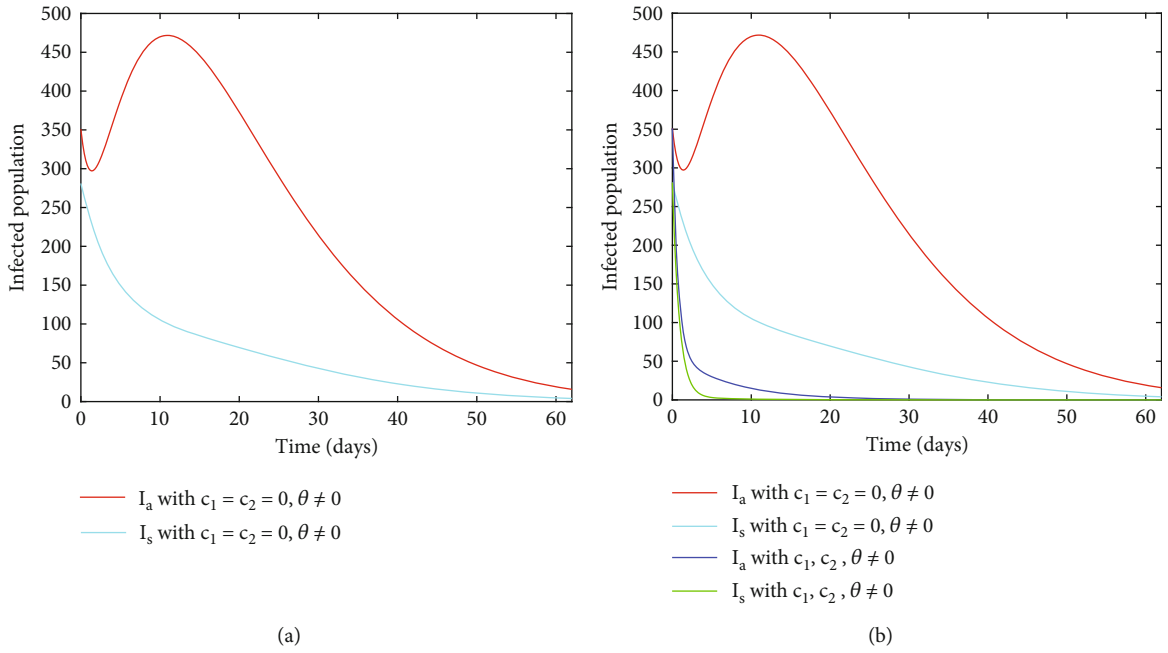

Figure 9: Solution curve depicting the impact of vaccine and control variables on infected humans.

7.3. Impact Control Strategies on $I_s(t)$. The effect of vaccination, preventative, and treatment control techniques on people with symptoms of infection is shown in Figure 6. As clearly depicted in Figure 6(a), the red line represents the controlled symptomatically infected humans with full dose vaccine and two control strategies, while the green line represents the controlled symptomatically infected individuals with full-dose vaccine only. This clearly indicates that the COVID-19 pandemic can be controlled fast if effective prevention, proper treatment, and vaccinations are carried out simultaneously. Moreover, if no control strategies are implemented, then symptomatically infested humans increases, as shown in Figure 6(b). Hence, we recommended that both dose vaccine, prevention, and treatment are essential to obtaining maximum protection from coronavirus.

7.4. Impact Control Strategies on $I_a(t)$. Figure 7 illustrates the impact of effective treatment, proper prevention, and vaccination on asymptotically infected humans with COVID-19. In Figure 7(a), the red line represents the controlled asymptomatically infected humans with full dose vaccine only, while the blue one shows the controlled asymptomatically infected humans with the use of full dose vaccine and the two control strategies simultaneously. The green solid line in Figure 7(b) shows that if no control strategies are used, then the rate of asymptotically infected individuals rises with time. This clearly indicates the COVID-19 pandemic can be controlled fast if effective prevention, proper treatment, and both shot vaccinations are carried out simultaneously. If the rate of the first dose of vaccination θ escalated from 0.11411 to 0.34110, then we observed that both symptomatically and asymptomatically infected cases decreased effectively, as shown in Figures 8(a) and 8(b).

Table 3: Sensitivity indices of $\mathfrak{R}_c$ for the proposed model.

Parameters	Sensitivity index
β	+Ve
ω	+Ve
ϕ_2	+Ve
ν	+Ve
ϕ_1	+Ve
γ_s	-Ve
γ_a	-Ve
ρ	-Ve
Φ	-Ve
α_a	-V
α_s	-V
θ	-Ve
μ	-Ve

7.5. Impact Control Strategies on $I_a(t)$ and $I_s(t)$. Figure 9 shows that asymptomatic infected individuals can spread the disease more than symptomatically infected individuals, and it is dangerous to control them relative to the symptomatic ones using control strategies like prevention and treatment. The first- and second-shot vaccine, i.e., θ, and ρ rate has a negative correlation to controlling the pandemic (see Figure 8 and Table 3). This led us to the conclusion that if we sufficiently enhance the vaccination rate for both doses and implement efficient preventive and appropriate treatment, the infection case in both symptomatic and asymptomatic instances may be significantly reduced. Generally,

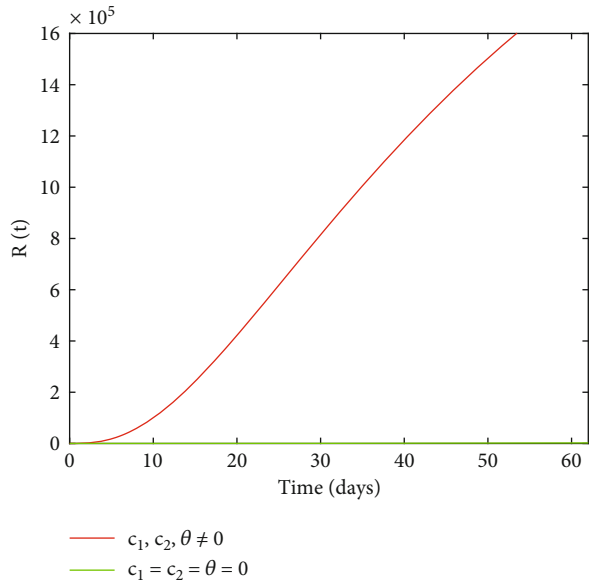

Figure 10: Impact of control strategies on recovered individuals.

from Figures 9(a) and 9(b), we conclude that asymptomatic individuals have a greater effect on the transmission of COVID-19 than the symptomatic one. In this stage, we can see that the number of cases in infected subgraphs dropped sharply after a few days, which also indicates that the combination of vaccination, personal protection, and treatment can effectively and quickly inhibit the distribution of the virus.

7.6. The Influence of Control Strategies on $R(t)$. Figure 10 shows that the recovered rate increases when full-dose vaccination, prevention, and treatment strategies are implemented simultaneously. But without thus controls, the number of recovered individuals is almost null. This reveals that the number of infectious averted humans from the COVID-19 pandemic due to the intervention of these controls observe that the biological interpretation of the model states that practicing the full dose vaccination and the two control strategies concurrently at the highest level from the beginning of the pandemic significantly minimized the number of cases in the populations to the extent that there are almost no cases, as shown in Figures 5–9, but Figure 10 shows the recovery rate increaseing.

8. Conclusion

With double dose vaccination and control strategies as prevention and treatment classes for the susceptible and infected populations, respectively, the newly emerged coronavirus transmission dynamics have been modeled and analyzed in this manuscript using non-linear order differential equations. Due to its human-to-human transmission method, COVID-19 encounters numerous difficulties worldwide and quickly spreads to become a pandemic. Therefore, in order to prevent this pandemic with limited resources, public health must be protected through appropriate vaccination as well as by enforcing any other control measures. In order to analyze the COVID-19 transmission dynamics using data that is readily available from Ethiopia, the $SV_1V_2EI_aI_sR$ compartmental disease model will be developed and mathematically examined. A mathematical model fitting to estimate the unknown parameters in our proposed model is also performed using real COVID-19 confirmed case data in Ethiopia from July 01, 2022, to August 31, 2022. We ran analytical and numerical simulations of the model provided using these parameters and identified two different equilibrium points: a disease-endemic equilibrium point and a disease-free equilibrium point. We also calculated the model's reproduction number in both the vaccine's presence and absence. We called this reproduction number the control reproduction number in the vaccine's presence, and we denoted it by $\mathfrak{R}_c$. The two equilibrium points of Equation (2) are locally and globally asymptotically stable are also shown. From the epidemiological perspective, we can draw the conclusion that the COVID-19 pandemic will approximately fade out of the population when $\mathfrak{R}_c < 1$; otherwise, it persists in society if $\mathfrak{R}_c > 1$. Therefore, the estimated $\mathfrak{R}_c$ for the suggested model utilizing the pandemic's reported cases can accurately ascertain the disease's true dynamics and identify the disease's current state in the Ethiopian population.

A sensitivity analysis has been performed to explore the effect of the model parameters on COVID-19 transmission dynamics. For instance, minimizing β and ω will highly help in reducing the infection burden in society. While boosting θ has a significant influence on decreasing the infection, employing θ and ρ jointly has a greater impact on minimizing the infection. The parameter β has 100% responsible for spreading the COVID-19 virus. Therefore, the effective transmission rate needs to be reduced in order to lessen the spread and burden of COVID-19 in the population. This can be accomplished by using the right preventative measures, such as health procedures like good personal hygiene, social seclusion, and the appropriate use of face masks.

This study draws special attention to controlling the transmission of the virus in society with the significance of first- and second-dose vaccination with other control strategies like perversion and treatment using real reported data in Ethiopia. Moreover, the impact of the first and second vaccine dose rate was demonstrated. Increasing vaccination rates has the predicted effect of reducing the number of infected people in the contaminated compartments. Increases in the second dose vaccination rate, in particular, have been shown to slow the spread of COVID-19 and control the endemic disease. However, COVID-19 continues to pose a hazard to the human population even after the first and second dose rates of the vaccine were implemented. Therefore, additional control measures, such as prevention and treatment for those who are most at risk of developing a significant COVID-19 illness, are necessary to further eradicate the disease in the population and stop the spread of another pandemic. The numerical simulation has demonstrated that both doses of vaccination have a negative impact on both symptomatic and asymptomatic cases. Therefore, from the numerical simulation and analytical analysis, we conclude that the use of both dose vaccination and control strategies such as treatment and perversion will highly eliminate the COVID-19 pandemic from the Ethiopian population.

Therefore, the output of this study can be used as a policy input for different countries with COVID-19 pandemic. In order to contain the disease, the World Health Organization (WHO) and nations around the world must implement a policy that requires that not only do full-dose vaccinations prevent pandemic outbreaks, but also that preventive measures and treatment are made necessary for all members of the population. The spread of COVID-19 can be greatly slowed down with a full-dose vaccine in conjunction with personal protection measures and aggressive treatment of affected patients. This will protect everyone on the planet from the deadly coronavirus of our generation.

Data Availability

The data used to support the findings of this study are in this paper.

Conflicts of Interest

It is stated by the authors that they have no competing interests.

Acknowledgments

All, the authors of the paper, acknowledge the Wallaga University Department of Mathematics for all the support through this work.

References

[1] M. Rafiq, J. Ali, M. B. Riaz, and J. Awrejcewicz, "Numerical analysis of a bi-modal COVID-19 sitr model," *Alexandria Engineering Journal*, vol. 61, no. 1, pp. 227–235, 2022.

[2] Anip Kumar Paul and Md Abdul Kuddus, "Mathematical analysis of a COVID-19 model with double dose vaccination in Bangladesh," *Results in Physics*, vol. 35, article 105392, 2022.

[3] A. Zeb, E. Alzahrani, V. S. Erturk, and G. Zaman, "Mathematical model for coronavirus disease 2019 (COVID-19) containing isolation class," *BioMed Research International*, vol. 2020, Article ID 3452402, 7 pages, 2020.

[4] C. Huang, Y. Wang, X. Li et al., "Clinical features of patients infected with 2019 novel coronavirus in Wuhan, China," *The Lancet*, vol. 395, no. 10223, pp. 497–506, 2020.

[5] J. D. A. Tyndall, "S-217622, a 3cl protease inhibitor and clinical candidate for sars-cov-2," *Journal of Medicinal Chemistry*, vol. 65, no. 9, pp. 6496–6498, 2022.

[6] H. Ritchie, E. Mathieu, L. Rodés-Guirao et al., "Coronavirus pandemic (COVID-19)," *Our World in Data*, vol. 2020, 2020.

[7] WHO Coronavirus, *Dashboard*, 2022, https://covid19.who.int/.

[8] A. Rajput, M. Sajid, Tanvi, C. Shekhar, and R. Aggarwal, "Optimal control strategies on COVID-19 infection to bolster the efficacy of vaccination in India," *Scientific Reports*, vol. 11, no. 1, pp. 1–18, 2021.

[9] E. Aruffo, P. Yuan, Y. Tan et al., "Community structured model for vaccine strategies to control COVID19 spread: a mathematical study," *PLoS One*, vol. 17, no. 10, article e0258648, 2022.

[10] L. Matrajt, J. Eaton, T. Leung, and E. R. Brown, "Vaccine optimization for COVID-19: who to vaccinate first?," *Advances*, vol. 7, no. 6, 2021.

[11] S. M. Kassa, J. B. H. Njagarah, and Y. A. Terefe, "Analysis of the mitigation strategies for COVID-19: _from mathematical modelling perspective_," *Chaos, Solitons & Fractals*, vol. 138, article 109968, 2020.

[12] P. N. A. Akuka, B. Seidu, and C. S. Bornaa, "Mathematical analysis of COVID-19 transmission dynamics model in Ghana with double-dose vaccination and quarantine," *Computational and Mathematical Methods in Medicine*, vol. 2022, Article ID 7493087, 10 pages, 2022.

[13] P. A. Naik, J. Zu, M. B. Ghori, and M.-u.-d. Naik, "Modeling the effects of the contaminated environments on COVID -19 transmission in India," *Results in Physics*, vol. 29, article 104774, 2021.

[14] Y. Cai, S. Zhao, Y. Niu et al., "Modelling the effects of the contaminated environments on tuberculosis in Jiangsu, China," *Journal of Theoretical Biology*, vol. 508, article 110453, 2021.

[15] P. A. Naik, M. Yavuz, S. Qureshi, Z. Jian, and S. Townley, "Modeling and analysis of COVID-19 epidemics with treatment in fractional derivatives using real data from Pakistan," *The European Physical Journal Plus*, vol. 135, no. 10, pp. 1–42, 2020.

[16] A. Atifa, M. A. Khan, K. Iskakova, F. S. Al-Duais, and I. Ahmad, "Mathematical modeling and analysis of the sars-cov-2 disease with reinfection," *Computational Biology and Chemistry*, vol. 98, article 107678, 2022.

[17] G. E. Mustafa, S. A. Abro, V. S. Zulkifli, N. M. Asirvadam, R. Kumar, and V. K. Oad, "Dynamic modeling of COVID-19 disease with impact of lockdown in Pakistan & Malaysia," in *2021 IEEE International Conference on Signal and Image Processing Applications (ICSIPA)*, pp. 156–161, Kuala Terengganu, Malaysia, 2021.

[18] F. Özköse and M. Yavuz, "Investigation of interactions between COVID-19 and diabetes with hereditary traits using real data: a case study in Turkey," *Computers in Biology and Medicine*, vol. 141, article 105044, 2022.

[19] O. J. Peter, H. S. Panigoro, A. Abidemi, M. M. Ojo, and F. A. Oguntolu, "Mathematical model of COVID-19 pandemic with double dose vaccination," *Acta Biotheoretica*, vol. 71, no. 2, 2023.

[20] S. S. Sharbayta, H. D. Desta, and T. Abdi, "Mathematical modelling of COVID-19 transmission dynamics with vaccination: a case study in Ethiopia," *medRxiv*, vol. 2023, 2022.

[21] Z. S. Kifle and L. L. Obsu, "Mathematical modeling for COVID-19 transmission dynamics: a case study in Ethiopia," *Results in Physics*, vol. 34, article 105191, 2022.

[22] A. A. Gebremeskel, H. W. Berhe, and H. A. Atsbaha, "Mathematical modelling and analysis of COVID-19 epidemic and predicting its future situation in Ethiopia," *Results in Physics*, vol. 22, article 103853, 2021.

[23] C. T. Deressa and G. F. Duressa, "Modeling and optimal control analysis of transmission dynamics of COVID-19: the case of Ethiopia," *Alexandria Engineering Journal*, vol. 60, no. 1, pp. 719–732, 2021.

[24] O. Diekmann, J. A. P. Heesterbeek, and J. A. J. Metz, "On the definition and the computation of the basic reproduction ratio r 0 in models for infectious diseases in heterogeneous populations," *Journal of Mathematical Biology*, vol. 28, no. 4, pp. 365–382, 1990.

[25] Firaol Asfaw Wodajo and Temesgen Tibebu Mekonnen, "Mathematical model analysis and numerical simulation of intervention strategies to reduce transmission and reactivation of hepatitis b disease," *F1000Research*, vol. 11, 2022.

[26] F. M. Legesse, K. P. Rao, and T. D. Keno, "Mathematical modeling of a bimodal pneumonia epidemic with non-breastfeeding class," *Applications of Mathematics*, vol. 17, no. 1, pp. 95–107, 2023.

[27] A. A. Gebremeskel, H. W. Berhe, and A. T. Abay, "A mathematical modelling and analysis of COVID-19 transmission dynamics with optimal control strategy," *Computational and Mathematical Methods in Medicine*, vol. 2022, Article ID 8636530, 15 pages, 2022.

[28] WHO COVID, *Dashboard*, World Health Organization, 2022, https://covid19.who.int.

[29] H. W. Berhe, "Optimal control strategies and cost-effectiveness analysis applied to real data of cholera outbreak in Ethiopia's Oromia Region," *Chaos, Solitons & Fractals*, vol. 138, article 109933, 2020.

[30] L. B. Dano, K. P. Rao, and T. D. Keno, "Modeling the combined effect of hepatitis b infection and heavy alcohol consumption on the progression dynamics of liver cirrhosis," *Journal of Mathematics*, vol. 2022, Article ID 6936396, 18 pages, 2022.

[31] C. T. Deressa, Y. O. Mussa, and G. F. Duressa, "Optimal control and sensitivity analysis for transmission dynamics of coronavirus," *Results in Physics*, vol. 19, article 103642, 2020.

[32] L. S. Pontryagin, V. G. Boltyanskii, R. V. Gamkrelidze et al., *Selected Works: The Mathematical Theory of Optimal Processes*, Routledge, 2018.

[33] D. Lee, M. A. Masud, B. N. Kim, and C. Oh, "Optimal control analysis for the MERS-CoV outbreak: South Korea perspectives," *Journal of the Korean Society for Industrial and Applied Mathematics*, vol. 21, no. 3, pp. 143–154, 2017.